

## RF-Sputtered Vanadium Oxide Thin Films: Effect of Oxygen Partial Pressure on Structural and Electrochemical Properties

Yong Joon Park,\* Nam-Gyu Park,\* Kwang Sun Ryu, Soon Ho Chang,  
Sin-Chong Park,† Seon-Mi Yoon,‡ and Dong-Kuk Kim‡

Battery Technology Team, Electronics and Telecommunications Research Institute(ETRI),  
161 Gajeong-Dong, Yuseong-Gu, Daejeon 305-350, Korea

†School of Engineering, Information and Communications University, 58-4, Hwaam-Dong,  
Yuseong-gu, Daejeon 305-732, Korea

‡Department of Chemistry, College of Natural Sciences, Kyungpook National University, Taegu 702-201, Korea  
Received May 25, 2001

Vanadium oxide thin films with thickness of about 2000 Å have been prepared by radio frequency sputter deposition using a V<sub>2</sub>O<sub>5</sub> target in a mixed argon and oxygen atmosphere with different Ar/O<sub>2</sub> ratio ranging from 99/1 to 90/10. X-ray diffraction and X-ray absorption near edge structure spectroscopic studies show that the oxygen content higher than 5% crystallizes a stoichiometric V<sub>2</sub>O<sub>5</sub> phase, while oxygen deficient phase is formed in the lower oxygen content. The oxygen content in the mixed Ar + O<sub>2</sub> has a significant influence on electrochemical lithium insertion/deinsertion property. The discharge-charge capacity of vanadium oxide film increases with increasing the reactive oxygen content. The V<sub>2</sub>O<sub>5</sub> film deposited at the Ar/O<sub>2</sub> ratio of 90/10 exhibits high discharge capacity of 100 μAh/cm<sup>2</sup>-μm along with good cycle performance.

**Keywords :** Vanadium oxide, Thin film, Microbattery, RF-sputtering.

### Introduction

Recently, thin film lithium secondary batteries have attracted much attention<sup>1-5</sup> due to their potential applications, such as MEMS (microelectromechanical system) devices, smart cards and small sensors. Thin film batteries are composed of thin film cathode, anode and solid electrolyte. Most of the studies for thin film secondary batteries have been focused on preparation and electrochemical properties of thin film electrodes. This is because the discharge-charge capacity of thin film battery is mainly dependent on electrode materials. As the cathode electrode for lithium battery, lithium cobalt oxide (LiCoO<sub>2</sub>), lithium manganese oxide (LiMn<sub>2</sub>O<sub>4</sub>) and vanadium oxide (V<sub>2</sub>O<sub>5</sub>) have been studied.<sup>6-9</sup> Among these, vanadium oxide is a promising material for the cathode of thin film battery due to its high discharge capacity and good cycle performance. Moreover, it can be prepared at room temperature by vacuum system such as sputtering and such a low-temperature preparation is of great beneficial to on-chip applications.

In the preparation of vanadium oxide films by radio frequency (RF) sputtering technique, the stoichiometry, structure and orientation of vanadium oxide can be influenced by the process parameters such as RF power, reactive gas atmosphere, temperature and substrate. The nature of vanadium oxide films can also affect their electrochemical properties. Therefore, a careful control is required to obtain high quality vanadium oxide thin films for battery application.

In this work, we have investigated an effect of reactive oxygen content in the mixed Ar + O<sub>2</sub> atmosphere on structural and electrochemical properties of vanadium oxide thin films prepared by radio frequency (RF) sputtering method.

### Experimental Section

Vanadium oxide thin films were deposited by radio frequency (RF) magnetron sputter using a V<sub>2</sub>O<sub>5</sub> target (4.25-inch diameter, CERAC, 99.9%) on a Si (100)/SiO<sub>2</sub> (2000 Å) /Pt (1000 Å) substrate at an ambient temperature. The target to substrate distance was 5 cm. The RF power and the total pressure during deposition were 100 W and 10 mTorr, respectively. The films were grown in a mixed Ar + O<sub>2</sub> atmosphere, where the argon flow rates were 70 ± 2 sccm and the oxygen flow rates of 0.7-7 sccm were controlled to give rise to the Ar/O<sub>2</sub> ratios of 99/1, 95/5 and 90/10. The thickness of the as-grown films were about 2000 Å as measured by a Tencor Alpha-step profiler.

X-ray diffraction analysis was performed using Rigaku X-ray diffractometer in the 2θ range from 5 to 60° with Cu-Kα radiation (λ = 1.5406 Å).

The V K-edge X-ray absorption near edge structure (XANES) spectra were recorded at beamline EXAFS3C1 at the Pohang Accelerator Laboratory (PAL), operated at 2.5 GeV with ca. 100-150 mA of stored current. A Si (311) double crystal monochromator was employed to collect high resolution XANES spectra. The absorption energy was calibrated by simultaneously measuring V K-edge XANES spectrum for vanadium metal foil. All XANES spectra were recorded in fluorescence mode. The data analyses for experimental spectra were performed by the following standard

\*Corresponding authors. Y.J.P.: Tel: +82-42-860-5516; Fax: +82-42-860-6836; e-mail: yjpark@etri.re.kr; N.G.P.: Tel: +82-42-860-5680; Fax: +82-42-860-6836; e-mail: npark@etri.re.kr

procedure. The inherent background in the data was removed by fitting a polynomial to the pre-edge region and extrapolated through the entire spectrum, from which it was subtracted. The absorption,  $\mu(E)$ , was normalized to an edge jump of unity.

Electrochemical characterization of the vanadium oxide thin films was carried out in a non-aqueous half-cell, two electrodes system, at ambient temperature using a Macpile II equipment. Active areas of vanadium oxide films for electrochemical test were about  $1 \times 1 \text{ cm}^2$ . A lithium foil and 1 M  $\text{LiClO}_4$  in propylene carbonate (PC) were used as an anode and an electrolyte, respectively. The cells were fabricated in dry room and tested galvanostatically at a constant current of  $10\text{--}100 \mu\text{A}/\text{cm}^2$ .

### Results and Discussion

The XRD patterns for the vanadium oxide films deposited at different  $\text{Ar}/\text{O}_2$  ratios are shown in Figure 1. The film deposited at low oxygen content, the  $\text{Ar}/\text{O}_2$  ratio of 99/1, shows only a peak at  $2\theta = 19.4^\circ$  with weak intensity that corresponds to neither  $\text{V}_2\text{O}_5$  nor  $\text{VO}_2$ . This unidentified peak may be associated with oxygen-deficient phase due to low oxygen atmosphere. On the other hand, the (001) diffraction peak corresponding to  $\text{V}_2\text{O}_5$  starts to appear when 5% oxygen is introduced, but mixed phase is still existed. For the case of the 10% oxygen-contained condition, a strong (001) peak is observed, indicating a formation of highly oriented  $\text{V}_2\text{O}_5$

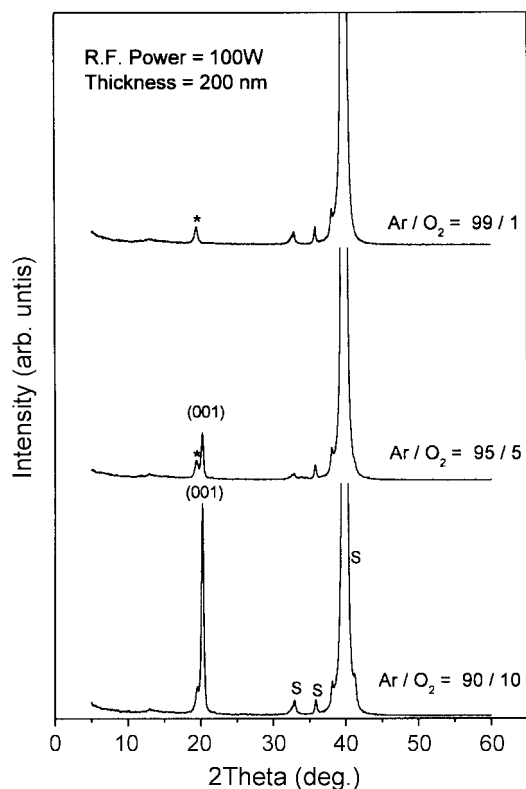


**Figure 1.** X-ray diffraction patterns for vanadium oxide films deposited at various  $\text{Ar}/\text{O}_2$  ratios. S and \* denote substrate peak and unidentified peak, respectively.

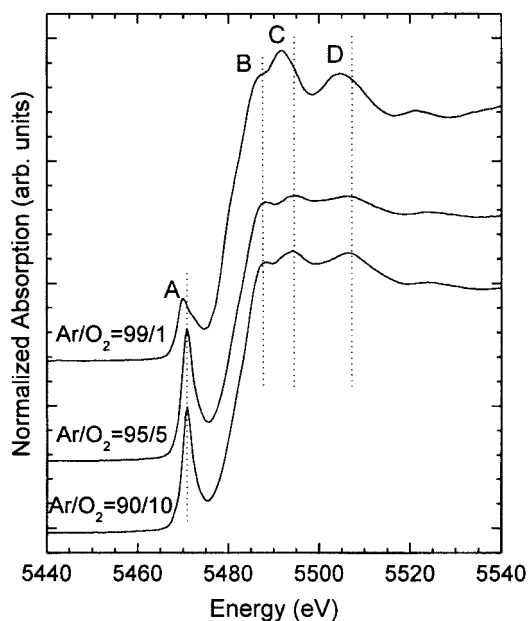


**Figure 2.** Normalized vanadium K-edge XANES spectra of vanadium oxide films deposited at various  $\text{Ar}/\text{O}_2$  ratios.

film with the  $ab$  plane parallel to the substrate. The layer structured  $\text{V}_2\text{O}_5$  film is similarly observed in the previous report.<sup>11</sup>

The XANES spectra of vanadium oxide thin films are recorded to investigate the oxidation state and local symmetry of vanadium. Figure 2 shows the V K-edge XANES spectra, in which pre-edge absorption feature (A) grows in intensity and shifts to higher energy upon the increase of oxygen content. It is well known that the intensity of pre-edge peak A, which is due to the transition from  $1s$  to  $3d$ , is proportional to the deviation from octahedral symmetry of the vanadium site.<sup>12-15</sup> In this respect, the change of intensity and position of pre-edge peak suggests that vanadium ion in the film deposited at the  $\text{Ar}/\text{O}_2$  ratio of 99/1 has higher symmetric local structure and lower oxidation state in comparison with that in the films deposited at the  $\text{Ar}/\text{O}_2$  ratio of 95/5 and 90/10. Especially, the difference of 0.2 eV in the position of pre-edge peak between the film deposited at the  $\text{Ar}/\text{O}_2$  ratio of 99/1 and other films is well consistent with the difference between the pre-edge peak positions observed at V K-edge XANES spectra for bulk oxides of  $\text{VO}_2$  and  $\text{V}_2\text{O}_5$ . Moreover, the XANES spectrum for the film deposited at the  $\text{Ar}/\text{O}_2$  ratio of 99/1 exhibits the representative spectral features of bulk  $\text{VO}_2$  with the slightly distorted octahedral local structure around vanadium ion in the overall spectral region from pre-edge to post-edges of B, C, and D. In the same manner, the XANES spectra for the films deposited at higher oxygen ratio have a strong resemblance to the overall spectral features of bulk  $\text{V}_2\text{O}_5$  with local structure of square pyramidal. As previously mentioned, X-ray diffraction method could not tell us a clear kind of material consisting of deposited film, which might be due to the lack of long-range ordered structure and/or highly oriented film structure. However, XANES spectra measured at V K-edge clearly suggest

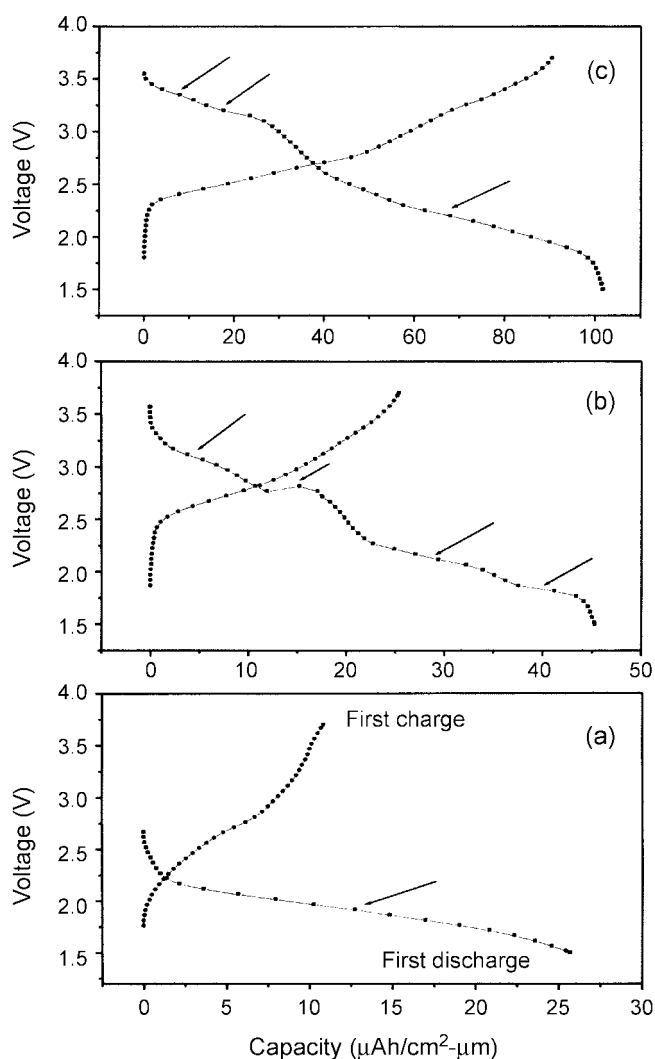


**Figure 3.** First discharge-charge profiles for the vanadium oxide films deposited at the Ar/O<sub>2</sub> ratio of (a) 99/1, (b) 95/5 and (c) 90/10. Data are collected at a constant current density of 100  $\mu\text{A}/\text{cm}^2$ . Arrows indicate plateau regions.

that materials consisting of film changes from VO<sub>2</sub> or VO<sub>2</sub>-like to V<sub>2</sub>O<sub>5</sub>, depending upon the oxygen partial pressure during sputtering process.

The first discharge-charge profiles of the vanadium oxide films deposited at various Ar/O<sub>2</sub> ratios are displayed in Figure 3. The current density for measurement is 100  $\mu\text{A}/\text{cm}^2$  that corresponds to about 4C rate. The film deposited at the Ar/O<sub>2</sub> ratio of 99/1 exhibits low open circuit voltage of 2.7 V and a plateau at 2.0 V in discharge curve (Fig. 3a). This is attributed to the low oxidation state of vanadium ion. The discharge profile is very similar to that of VO<sub>1.88</sub> reported in previous report.<sup>16</sup> While, the film deposited at the Ar/O<sub>2</sub> ratio of 90/10 (Fig. 3c) exhibits stepwise discharge curve with three plateaus at about 3.35, 3.2 and 2.3 V, which is in accordance with previous report on crystalline V<sub>2</sub>O<sub>5</sub>.<sup>6</sup> The three plateaus imply  $\alpha + \epsilon$ ,  $\epsilon + \delta$  and  $\delta + \gamma$  phase mixtures, respectively. In the case of the film deposited at the Ar/O<sub>2</sub> ratio of 95/5, the four plateaus at 3.0, 2.7, 2.3, and

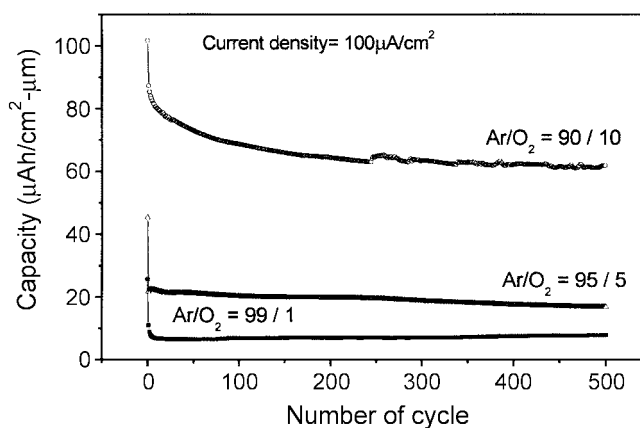


**Figure 4.** Cyclic performance for vanadium oxide films deposited at various Ar/O<sub>2</sub> ratios. Data are collected at a constant current density of 100  $\mu\text{A}/\text{cm}^2$ .

1.9 V are observed. As observed in XRD and XANES spectra, the mixed phase with a V<sub>2</sub>O<sub>5</sub> phase and a VO<sub>2</sub>-like phase obtained from the 5% O<sub>2</sub>-contained condition might result in the multi-plateaus in discharge process.

The discharge capacity increases with increasing the oxygen content as can be seen in Figure 3. The first discharge capacities of the films deposited at the Ar/O<sub>2</sub> ratio of 99/1 and 95/5 are only 26  $\mu\text{Ah}/\text{cm}^2\text{-}\mu\text{m}$  and 45  $\mu\text{Ah}/\text{cm}^2\text{-}\mu\text{m}$ , respectively, which is significantly improved to over 100  $\mu\text{Ah}/\text{cm}^2\text{-}\mu\text{m}$  when the film deposited at the Ar/O<sub>2</sub> ratio of 90/10. For the first charge capacity, merely 40 and 55% of the first discharge capacity are recovered for the films deposited at the Ar/O<sub>2</sub> ratio of 99/1 and 95/5, respectively, indicating a poor reversibility for lithium ion insertion/deinsertion. However, the film deposited at higher oxygen flow rate exhibits the charge capacity corresponding to about 90% of the first discharge capacity.

Figure 4 shows the capacity as a function of number of cycle. The capacity abruptly decreases during the first cycle, which is attributed to irreversible phase for lithium ion insertion/deinsertion formed during the first cycle. The capacity loss of our vanadium oxide films is similarly observed for the case of crystalline vanadium oxide powder, in which the irreversible phase transformation from  $\alpha$ -V<sub>2</sub>O<sub>5</sub> to  $\omega$ -Li<sub>x</sub>V<sub>2</sub>O<sub>5</sub> via  $\epsilon$ ,  $\delta$ ,  $\gamma$ -phases accounts for the capacity loss at initial discharge-charge process.<sup>6</sup> The films deposited at the Ar/O<sub>2</sub> ratio of 99/1 and 95/5 show very constant capacities after initial capacity loss, while the film deposited at the Ar/O<sub>2</sub> ratio of 90/10 shows a gradual decrease in capacity during 100 cycles and then retains almost constant capacity values. The capacity after 500 cycles is about 60  $\mu\text{Ah}/\text{cm}^2\text{-}\mu\text{m}$  for the film deposited at 10% oxygen.

## Conclusions

Vanadium oxide films have been deposited by RF sputtering method using a V<sub>2</sub>O<sub>5</sub> target in a mixed Ar + O<sub>2</sub> atmosphere. Low oxygen content in the mixed Ar + O<sub>2</sub> atmosphere, less than 5% oxygen at least in our experimental condition,

is found to be insufficient to form the  $V_2O_5$  crystalline phase, even though a  $V_2O_5$  target is used. Almost pure crystalline  $V_2O_5$  phase is formed at the 90% argon and 10% oxygen atmosphere. Oxygen partial pressure during film preparation condition has a significant influence on electrochemical performance. Films deposited at relatively low oxygen atmosphere exhibit a poor electrochemical property for lithium insertion/deinsertion. On the other hand, the film deposited at 10% oxygen-contained condition shows better electrochemical performance. From the current tests, we propose that the deposition condition of 90% argon and 10% oxygen atmosphere is desirable to produce a  $V_2O_5$  thin film cathode from a  $V_2O_5$  target.

**Acknowledgment.** This work was supported by the Korea Ministry of Informations and Communications (MIC).

### References

1. Bates, J. B.; Dudney, N. J.; Neudecker, B. J.; Ueda, A.; Evans, C. D. *Solid State Ionics* **2000**, *135*, 33.
  2. Park, Y. J.; Kim, J. G.; Kim, M. K.; Chung, H. T.; Kim, H. G. *Solid State Ionics* **2000**, *130*, 203.
  3. Neudecker, B. J.; Dudney, N. J.; Bates, J. B. *J. Electrochem. Soc.* **2000**, *147*, 517.
  4. Bates, J. B.; Gruzalski, G. R.; Dudney, N. J.; Luck, C. F.; Yu, X. *Solid State Ionics* **1994**, *70/71*, 619.
  5. Jones, S. D.; Akridge, J. R.; Shokoohi, F. K. *Solid State Ionics* **1994**, *69*, 357.
  6. Koike, S.; Fujieda, T.; Sakai, T.; Higuchi, S. *J. Power Sources* **1999**, *81-82*, 581.
  7. Park, Y. J.; Kim, J. G.; Kim, M. K.; Kim, H. G.; Chung, H. T.; Park, Y. *J. Power Sources* **2000**, *87*, 69.
  8. Polo Da Fonseca, C. N.; Davalos, J.; Kleinke, M.; Fantini, M. C. A.; Gorenstein, A. *J. Power Sources* **1999**, *81-82*, 575.
  9. Park, Y. J.; Kim, J. G.; Kim, M. K.; Chung, H. T.; Um, W. S.; Kim, M. H.; Kim, H. G. *J. Power Sources* **1998**, *76*, 41.
  10. McGraw, J. M.; Bahn, C. S.; Parilla, P. A.; Perkins, J. D.; Readey, D. W.; Ginley, D. S. *Electrochimica Acta* **1999**, *45*, 187.
  11. Kumagai, N.; Kitamoto, H.; Baba, M.; Durand-vidal, S.; Devilliers, D.; Groult, H. *J. Appl. Electrochem.* **1998**, *28*, 41.
  12. Giorgetti, M.; Passerini, S.; Smyrl, W. H.; Mukerjee, S.; Yang, X. Q.; McBreen, J. *J. Electrochem. Soc.* **1999**, *146*, 2387.
  13. Passerini, S.; Smyrl, W. H.; Berrettoni, M.; Rossici, R.; Rosolen, M.; Marassi, R.; Decker, F. *Solid State Ionics* **1996**, *90*, 5.
  14. Wong, J.; Lyte, F. W.; Messmer, R. P.; Maylotte, D. H. *Phys. Rev. B* **1884**, *30*, 5596.
  15. Gioretti, M.; Passerini, S.; Smyrl, W. H.; Berrettoni, M. *Chem. Mater.* **1999**, *11*, 2257.
  16. Abraham, K. M.; Goldman, J. L.; Dempsey, M. D. *J. Electrochem. Soc.* **1981**, *128*, 2493.
-